We are IntechOpen,
the world's leading publisher of
Open Access books
Built by scientists, for scientists

4,800
Open access books available

122,000
International authors and editors

135M
Downloads

Our authors are among the

154
Countries delivered to

TOP 1%
most cited scientists

12.2%
Contributors from top 500 universities

WEB OF SCIENCE™

Selection of our books indexed in the Book Citation Index
in Web of Science™ Core Collection (BKCI)

Interested in publishing with us?
Contact book.department@intechopen.com

Numbers displayed above are based on latest data collected.
For more information visit www.intechopen.com

UHF RFID of People

Milan Polívka, Milan Švanda and Přemysl Hudec
Czech Technical University in Prague
Czech Republic

1. Introduction

Recently, the application of RFID systems is more and more extended on monitoring and identifying people, both in indoor and outdoor areas. This application concerns, for example, monitoring of employees in offices working with sensitive information, in large factories or power plants, personnel in an army storehouse, supervisors in prisons, or long distance runners at checking gates. In all of these cases it can be important to know who is where. Identification can be combined with fast access. The approved people can be allowed to enter specific rooms or an area, non-approved can be restricted from entering. All of this can be carried out over a moderate distances without the person having to worry or perform any action.
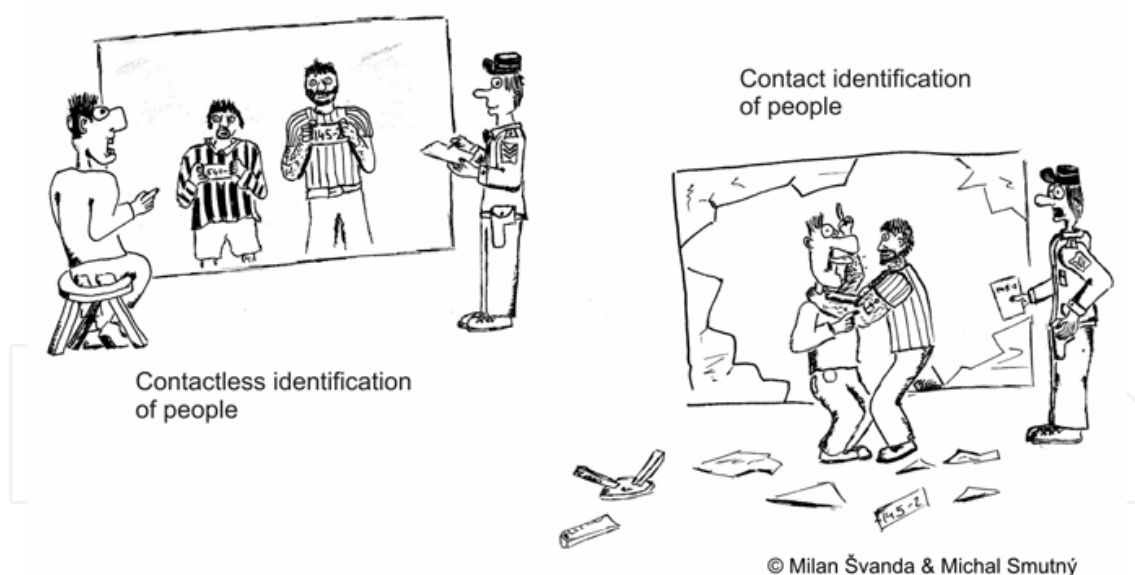

Fig. 1. Contactless and contact identification of people from the cartoonist's point of view

The identification distance of many RFID systems is relatively short, typically from several cm up to 1 m. This necessarily need not be a problem at a door access, but brings too many complications in wider corridors or open areas. For these purposes, it is important to identify the person at longer distances, convenient ranges can be from 2 to 10 m. For RFID purposes, a relatively wide range of frequencies is available. Operating frequencies used can be chosen in the low frequency band (LF, 125 kHz), high frequency band (HF, 13.56 MHz), ultra high frequency band (UHF, 860 - 930 MHz) or microwave bands (up to now

dominantly 2.4 GHz). LF and HF RFID systems can be used for monitoring of people, the problem is that only over a relatively short identification distance. The main reason for that, is the coupling used between the reader and TAGs. At these frequencies, standard antennas are too large and have too low gain. That is why a simple inductive coupling is used and that is why LF and HF RFID systems can only provide a short identification distance, typically up to 1 m (Finkenzeller, 2003). The person to be identified must come into a narrow vicinity of the reader or even touch the reader. The UHF and microwave RFID systems can use standard matched antennas and electromagnetic wave propagation as a coupling mechanism. Antennas at these frequencies can have acceptable dimensions and gains and identification systems can provide the required 2 - 10 m maximum identification distance. That is why UHF and microwave RFID systems seem to be very good candidates for monitoring of people over moderate distances.

For these purposes, standard UHF RFID systems can be used, but without careful design, they can lead to relatively poor results. Efficient and reliable monitoring and identification of people in large buildings is influenced by a number of specific conditions and physical phenomena. Above all, this concerns the operating frequency, the behavior of propagating electromagnetic waves at this frequency and the specific parameters of the antennas used.

The principal conditions for correct identification can be described in a form of two power budgets. The area to be monitored is illuminated by a TX reader antenna. The person to be monitored wears a TAG including its own receiving/transmitting antenna. The RF power received by the TAG antenna must be higher than the TAG sensitivity. This power enables the TAG to transmit (reflect) back a wave bearing the identification code. The power of this wave at the input of the reader receiver must be higher than its own sensitivity. Both power budgets are influenced by the RF power transmitted by the reader, by the gains of all antennas, by the free-space loss between the reader antenna and the TAG antenna and by additional losses specific to the propagation of electromagnetic waves under the given conditions. This above all concerns multi-path fading and shadowing. These additional power losses must be described and evaluated and taken into account during system calculations. To a definite degree, they can be minimized by system optimization and setting.

As it has been already mentioned, in the UHF and microwave bands, standard antennas with impedance matching and positive dB gain values can be used. Since higher frequencies lead to smaller antennas, it may be seen to be beneficial to use a microwave band. It is true, but it also must take into account that higher frequencies lead to higher values of free-space loss. So UHF operational frequency can also be a very good choice.

Usually, the choice of reader antenna represents no substantial problem. Any antenna with an acceptable radiation pattern and gain can be used. However, in some cases it can be beneficial to use the antennas with higher directivity that enables one to focus the energy to the expected identification area and improve both the power budgets. More problems are usually associated with TAG antennas as they represent the biggest part of the TAG. For the identification of people, the TAG must be worn, and that is why they must be as small and lightweight as possible. The design of very small antennas is a problem by itself, due to the principal limitations. But an additional problem lies in the fact that the parameters of the majority of the standard RFID antennas are strongly affected by a nearby presence of a human body. The body can detune the antenna and absorb a substantial part of the received

or transmitted RF power. Both phenomena can strongly affect power budgets and result in a wrong identification.

Efficient and reliable monitoring and identification of people in large buildings or outdoor areas belongs to a relatively difficult technical task. These difficulties are dominantly associated with operating frequency, with the behavior of the electromagnetic waves in the given frequency band and with the antennas used. All of these problems must be carefully solved and each RFID system must be "tuned" for the given application. The following sections include more detailed treatment of all of the above described problems.

2. TAG antennas for UHF RFID of people

The design of a UHF TAG antenna suitable for monitoring of people has several important requirements. Some of them are slightly different from demands made on standard communication antennas, this especially concerns:

- Impedance matching to complex impedance different from 50 Ω
- Immunity of antenna parameters from the nearby presence of a human body
- Small dimensions and weight, sometimes also flexibility

RFID chip impedances usually have a capacitive component (Finkenzeller, 2003) that is why, in order to ensure the impedance matching, the input impedance of the TAG antenna has to provide the corresponding inductive component. In the case of standard RFID dipole antennas, this inductive component is often realized by a small parallel loop (Sidén et al., 2006).

Furthermore, the design of the intended UHF TAG antennas has to take into account the close vicinity of a human body. In UHF band that represents a high-loss dielectric object with a relative permittivity $\varepsilon_r \sim 50 - 60$ and loss tangent $\tan \delta \sim 0.5 - 1.2$ (Gautherie, 1990). In case of the dipole type TAG antennas, the presence of such dielectric causes significant detuning and absorption of the radiated or received energy (Foster & Burberry, 1999), (Raumonen et al., 2003), (Dobkin & Weigand, 2005), (Griffin et al., 2006). This results in a low radiation efficiency and consequently in a short identification distance. Thus, antenna structures immune to an undesirable influence of a human body together with a small footprint, and a low profile are highly recommended (Ukkonen & Kivikoski, 2003).

The problem of frequency detuning and energy absorption can be, on principle, solved by insertion of a screening metallic plate. The plate can act as an additional shielding or can form an inherent part of the TAG antenna. The first following section concerns the problems of the operation of the standard dipole antennas above the metallic plane. The original solution using multiple-arm dipoles is presented. The other section describes the TAG antennas, newly designed especially for identification of people that employ metallic plates as an inherent part of their structures. All new TAG antennas were designed with respect to minimization of their profile, which is important for realization of wearable antennas. All were impedance matched at 869 MHz to the RFID chip described in Table 3.

2.1 Dipole type antennas

Dipole type antennas, for their simple design and manufacturing, are the natural and usual choice for TAG antennas in the UHF and microwave bands. To be able to efficiently radiate electromagnetic waves, their sizes have to be comparable with the half- or quarter-wavelength (approx. 160 - 170 and 80 - 85 mm in the UHF band, respectively). In case of any miniaturized version, such as the meander-shortened dipole, the radiation resistance

(Noguchi et al., 1997) and consequently the radiation efficiency and identification distance can decrease significantly. Unfortunately, electrical properties of this type of antenna are also very sensitive to any dielectric or metallic object situated in its near proximity. In the case of a closely spaced metallic plane, out-phase image currents induced in the plane decrease the antenna input resistance and consequently also the radiation efficiency. Thus, in order to operate efficiently, the dipoles usually require a relatively thick space pad (Ranasinghe et al., 2004), (Sidén et al., 2006).

In order to demonstrate impedance and radiation properties of a dipole closely spaced to a metallic plane, a planar dipole according to Fig. 2a is considered.

As it can be seen, the lower the relative distance h/λ_0 is, the lower the input impedance is, see Fig. 2b.

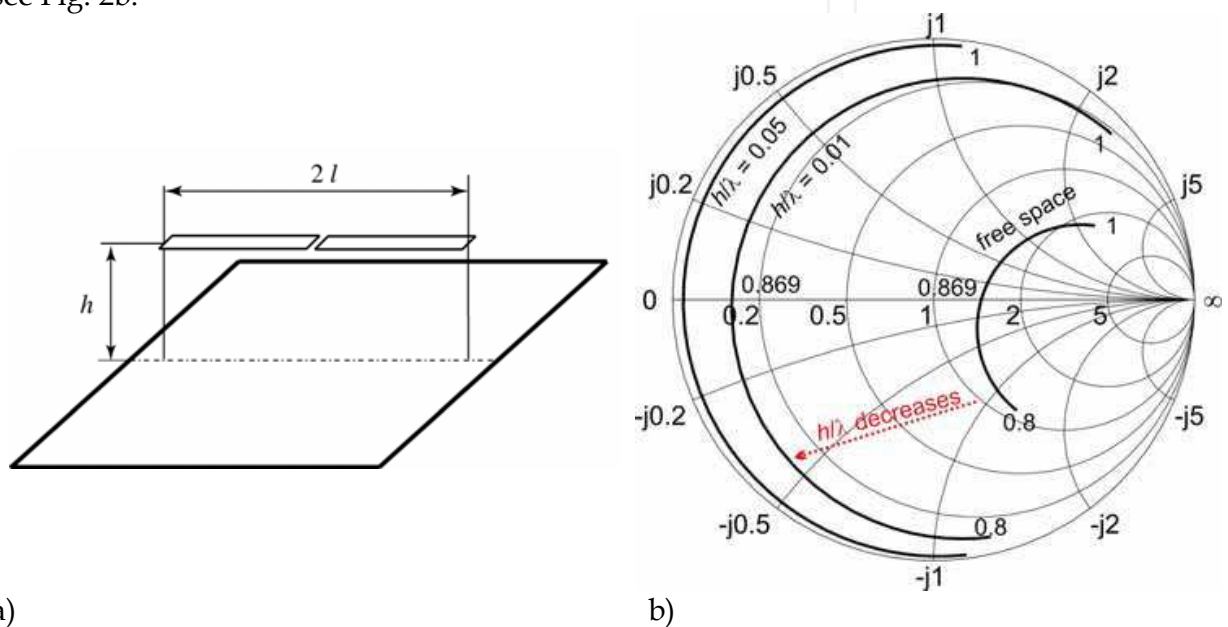a)   b)

Fig. 2. Geometry of a planar dipole, length $2l$ = 163.3 mm and width w = 2 mm placed above an infinite conductive plane a) and b) its input impedance curves in the Smith chart for the frequency range from 0.8 to 1.0 GHz as a function of the relative dipole distance over the conductive plane ($h/\lambda_0 = \infty$ (free space), 0.01, 0.005).

On the contrary to the decrease of the antenna efficiency, the decline of the radiation efficiency is not so progressive; see Fig. 3. As far as $h \geq 0.01\,\lambda_0$ (~ 3.5 mm at 869 MHz) the radiation efficiency is still slightly above 20 %, while the antenna efficiency due to the impedance mismatch (related to standard 50 Ω) drops to 1 - 2 %.

One of the possible ways how to increase the low input resistance of a dipole closely spaced above a metallic plane is to use the multiple-conductor (arm) folded dipole configuration (Best, 2004). The physical relation of the input impedance Z_{in} and the number N_{arm} of the dipole arms in the half wavelength, the multiple-arm folded dipole configuration may be expressed as follows (Balanis, 1997):

$$Z_{in} \approx N^2{}_{arms} Z_{11} \tag{1}$$

where Z_{11} is the self impedance of a single dipole. However, it is necessary to point out that the above-mentioned relation is uniquely valid provided that the dipoles are closely spaced and the magnitudes of all dipole currents are supposed to be the same. The effect of
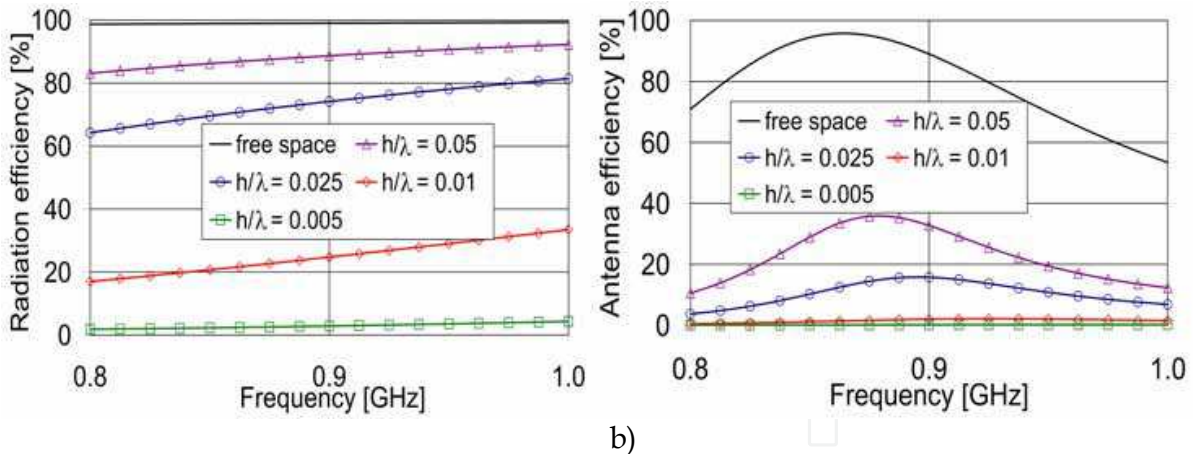
Fig. 3. Simulated frequency dependencies of the a) radiation and b) antenna efficiencies of a planar dipole as a function of the relative distance h/λ_0 = {free space, 0.05, 0.025, 0.01, 0.005}

decreasing dipole Z_{in}, when closely spaced to a metallic plane, is thus compensated by the increase of Z_{in} caused by the multiple-arm folded dipole configuration. This results in an approximate linear dependence of $Z_{in} = f(N_{arms})$ as verified by the results of the EM field simulations (Polívka et al., 2008a). Using the operation in an inductive region above the half-wavelength resonance, a impedance matching of the imaginary part of the TAG antenna to the imaginary part of the RFID chip impedance can be easily achieved; see Fig. 4b. The same figure shows the increase in the input resistance of the multiple-arm folded dipole according to Fig. 4a as a function of the number N_{arms}, details can be found in (Polívka et al., 2008a). The simulated results corresponding to N_{arms} = 33 show approx. 50 % radiation and antenna efficiencies; see Fig. 5.
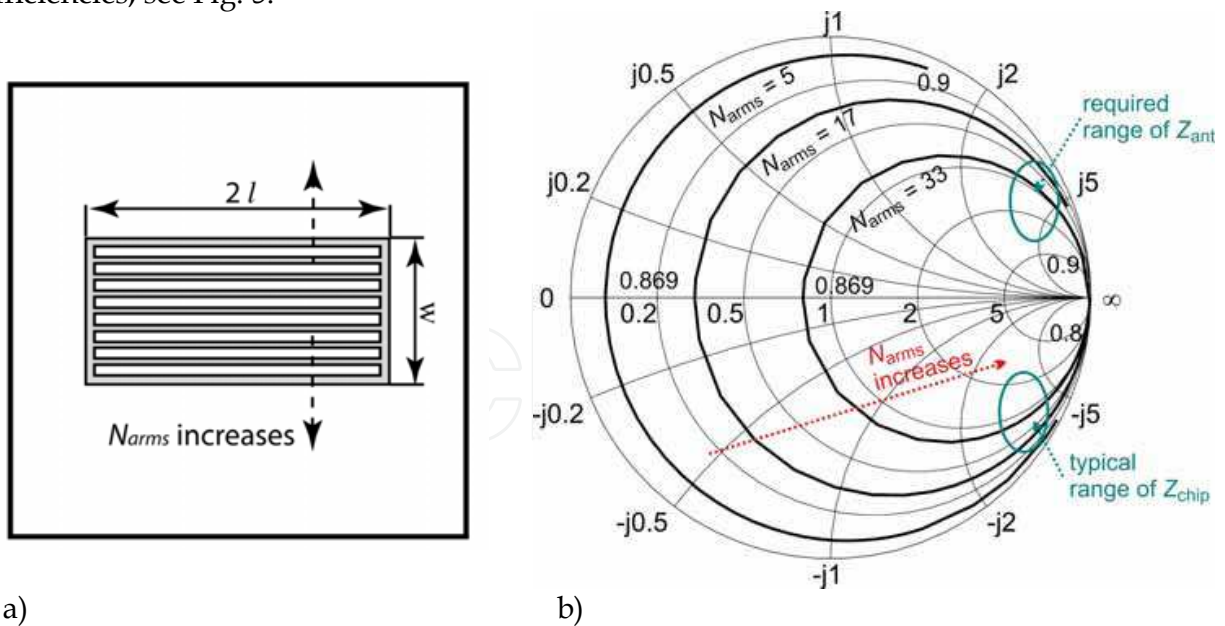

Fig. 4. The geometry of the multiple-arm folded dipoles with dipole length $2l$ = 134 mm, width w = 98 mm, spacing of arms s = 1 mm, spaced $h/\lambda_0 \sim 0.003$ (d = 1.04 mm consisting of a 0.8 mm thin foam substrate and 0.24 mm thin GML 1100 woven-glass laminate) over a test metallic plane of size 242 × 120 mm a) and their input impedance in a Smith chart in the frequency range 0.8 - 1.0 GHz b) as a function of the number of arms (N_{arms} = 1, 5, 17, 33).

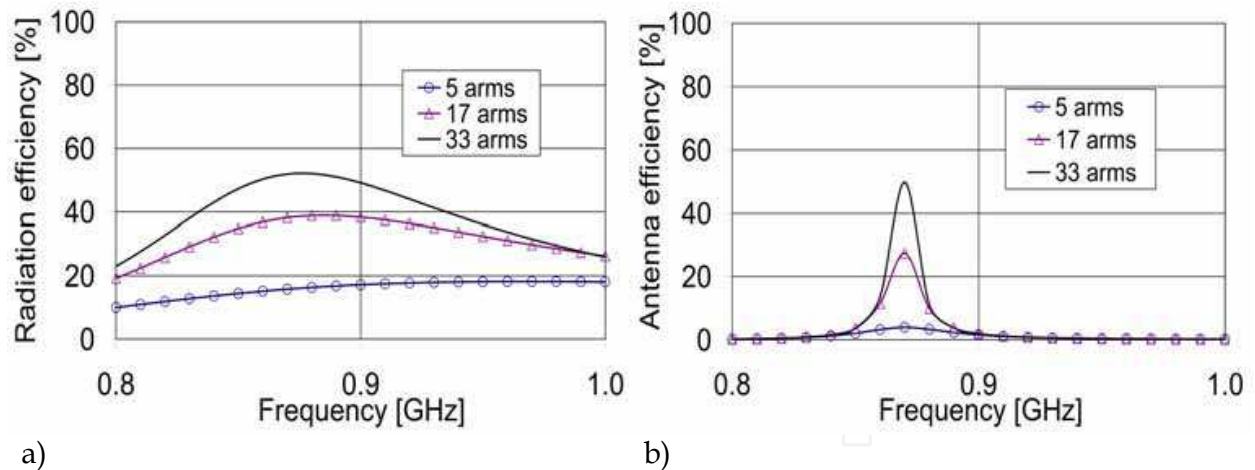a)   b)

Fig. 5. The simulated a) radiation and b) antenna efficiency of the multiple-arm folded dipole from Fig. 4 (at f_0 = 869 MHz) as a function of the frequency with spacing h/λ_0 over the metallic plane as the parameter.

The main advantage of this solution is an extremely low achievable profile ($h/\lambda_0 \sim 0.003$). The drawbacks are a relatively large footprint size ($\sim 0.4 \times 0.3\ \lambda_0$) and narrow operational bandwidth. But in the case of narrowband RFID applications, where antenna dimensions are not a limiting requirement, this multiple-arm folded dipole structure can provide the TAG antenna with acceptable parameters.

2.2 Patch and PIFA antennas

PIFA (Ukkonen et. al., 2004), (Hirvonen et. al., 2004) and patch (Ukkonen et al., 2005), (Švanda et al., 2007), (Švanda & Polívka, 2007) antennas represent radiating structures where the metallic ground plane is their inherent part. However, at relatively low operational frequencies (hundreds of MHz and lower), several potential difficulties must be taken into account. Firstly, when the substrate height is lower than $\sim 0.01\ \lambda_0$, and relative permittivity ε_r is higher than that of the air or foam substrate, see Fig. 6, their radiation efficiency decreases significantly (Lee & Chen, 1997). Secondly, the basic patch resonant
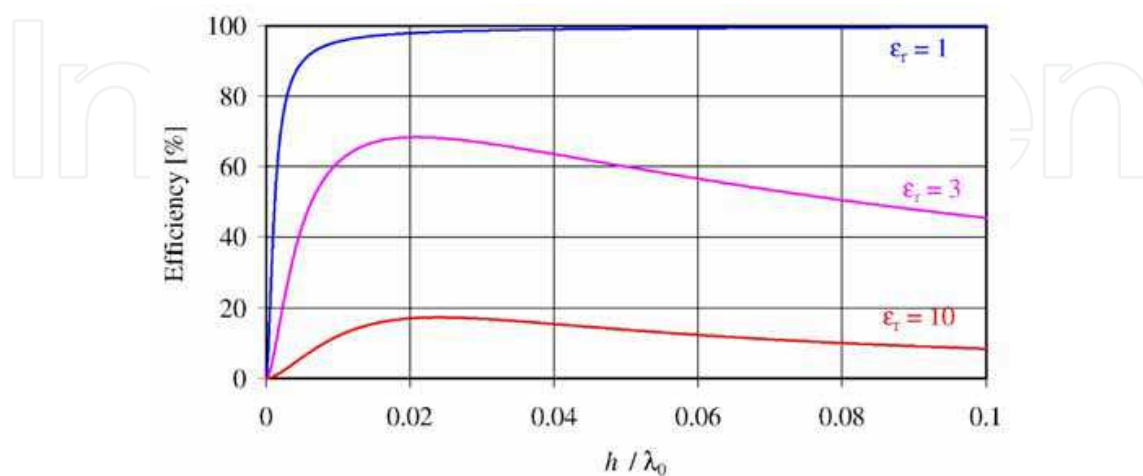

Fig. 6. Radiation efficiency as a function of the relative substrate height, according to (Lee & Chen, 1997)

frequency corresponds to $\lambda_0/2$ or $\lambda_0/4$ and, therefore, at UHF frequencies, the patch or PIFA antennas might not be sufficiently small for the intended application. However, in definite applications of person identification, larger patch antenna footprints need not be the most limiting parameter. For example, this concerns the identification of long distance racers in a more detailed way described in Section 3.4.1. where nearly $\lambda_0/2$ low profile and very lightweight antennas were integrated into their number labels.

This new RFID patch antenna (Švanda et al., 2007), see Fig. 7, was fabricated on a foam dielectric (G3 9568 foam $h = 4.8$ mm, $h/\lambda_0 \sim 0.014$) using a conductive fabric. The ground plane dimensions are 165×74 mm, the measured gain of an antenna placed on a human body is 5.0 dBi. The weight of the antenna is approx. equal to 20 g, it is flexible and, as it was mentioned before, it was easily integrated into the sportsmens' number labels.
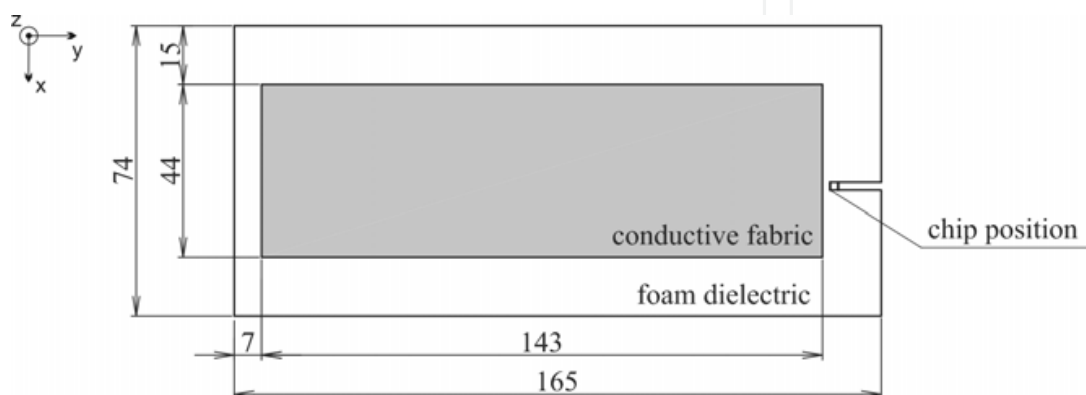

Fig. 7. Sketch of designed prototype of the patch TAG antenna

The comparison of the gains of the RFID patch antenna measured in a free space and on a human body phantom (a tank with 5 liters of salt water) is presented in Table 1. The parameter b represents the distance between the antenna and the phantom. Fig. 8 shows the measured radiation patterns in free space and fixed on the phantom and indicates the very low influence of a nearby human body on the antenna parameters.

	G [dBi]	D [dBi]	η [%]
free space	6.3	6.7	91
$b = 0$ mm	5.0	7.6	55

Table 1. Measured gain, directivity, and antenna efficiency of a patch TAG antenna

2.3 Small flat-loop antenna loaded by a sub-wavelength patch array backed by grounded dielectric slab

Generally, as electrical small loop antennas provide inductive input impedance (Hansen, 2006), they seem to be good candidates for RFID TAG applications. However, the properties of the loop antenna highly depend on the pad material, moreover the loop perimeter is comparable to the wavelength. If the circular loop is flattened to a low oval, its length is close to about a half-wavelength. Both of the above-mentioned problems can be eliminated by using a grounded substrate with relatively high permittivity ($\varepsilon_r \sim 10$). Due to the dielectric slab used, the loop size gets significantly smaller. There still remains a problem with the radiation efficiency, which drops in case of the thin substrate thickness (up to ~ 1.5 mm) to about 17 %; see Fig. 10. This phenomenon is caused by destructive interferences among the reflected and transmitted waves (Sievenpiper, 1999). Artificial
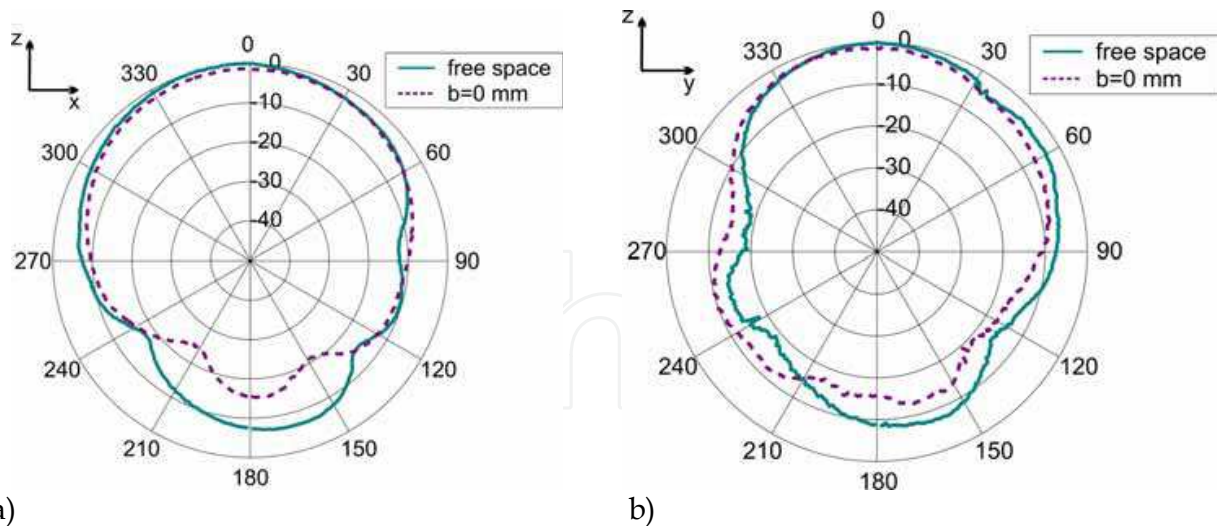
Fig. 8. Measured radiation patterns of a patch antenna a) H-plane b) E-plane

magnetic conductors (Zhang et al., 2003) were a certain inspiration for designing a four-element sub-wavelength patch array backed by a grounded dielectric slab. This slab was used as a screening plane for a small flat dual-loop antenna (Švanda & Polívka, 2008); see Fig. 9. This solution minimizes the resulting antenna size, the dual-loop footprint is 70 × 11 mm. The total antenna size including the backing patch array etched on a 1.58 mm ($h/\lambda_0 \sim 0.005$) thick grounded dielectric substrate is 70 × 105 × 1.82 mm (relative size is 0.2 × 0.3 × 0.005 λ_0 at 869 MHz). The reason for using the dual-loop modification is to increase the real part of the antenna input impedance.
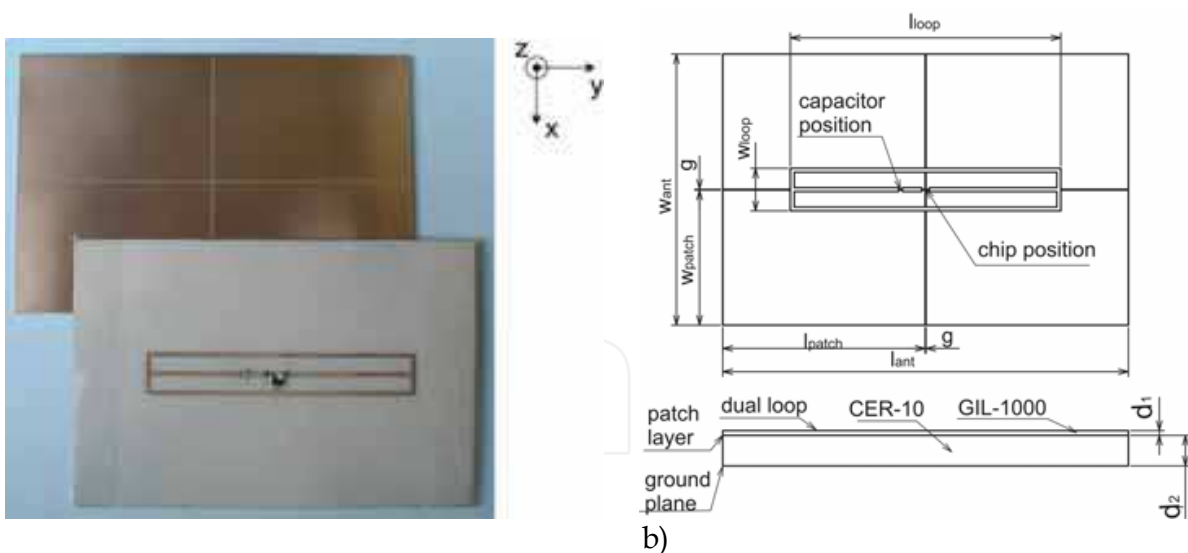

Fig. 9. Photograph a) and drawing b) of the designed prototype of the flat dual-loop antenna closely spaced over a patch array surface, $d_1 = 0.24$ mm, $d_1/\lambda_0 \sim 0.0007$, $\varepsilon_{r1} \sim 3.05$, $d_2 = 1.58$ mm, $d_2/\lambda \sim 0.0046$, $\varepsilon_{r2} \sim 10$. The total relative dimensions are 0.2 × 0.3 × 0.005 λ_0 at 869 MHz.

The comparison of the radiation efficiency of the flat single loop antenna in the free space, above the metallic plane, and above the four-element patch array etched on the grounded dielectric slab can bee seen in Fig. 10.
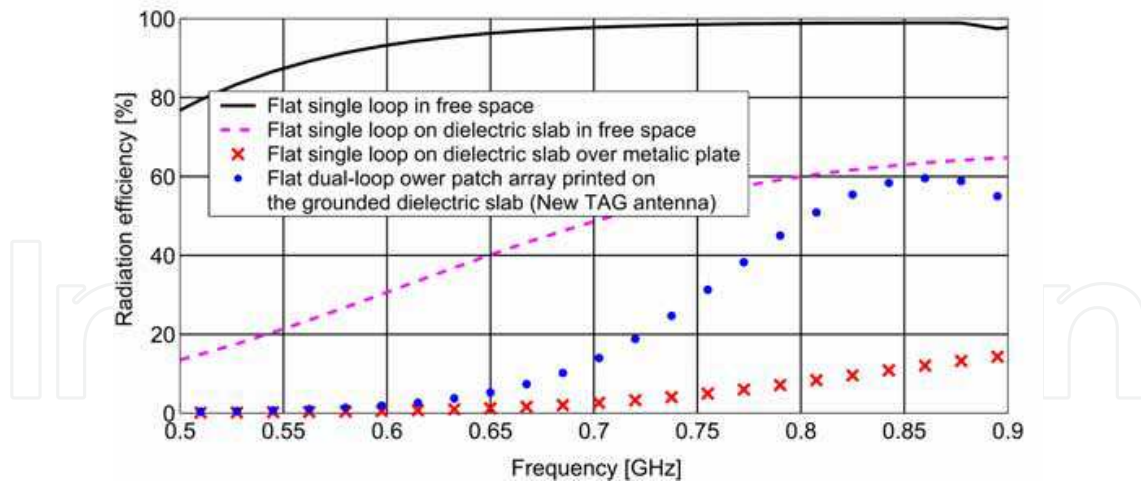
Fig. 10. Comparison of the simulated radiation efficiency for the different versions of flat loop antennas

In order to enable the measurement of the antenna input impedance, a half-loop (equivalent to the monopole) arrangement equipped an SMA connector was designed and realized; see Fig. 11a. The size of the mirror metallic plane is 145 × 145 mm. The half-loop antenna input impedance should have a half value of the loop antenna input impedance. The power transmission coefficient τ is calculated by means of the following equation:

$$\tau = 1 - |\Gamma|^2 = \frac{4 R_{ant} R_{chip}}{\left(R_{ant} + R_{chip}\right)^2 + \left(X_{ant} + X_{chip}\right)^2}, \quad 0 \le \tau \le 1 \tag{2}$$

$$\Gamma = \frac{Z_{chip} - Z_{ant}}{Z_{chip} + Z_{ant}}, \quad 0 < |\Gamma| < 1 \tag{3}$$

where Γ is the reflection coefficient between the antenna and the chip impedances, R_{ant} and R_{chip} represent the antenna and the chip input resistances, X_{ant} and X_{chip} stand for the antenna and the chip input reactance, respectively.

a)   b)
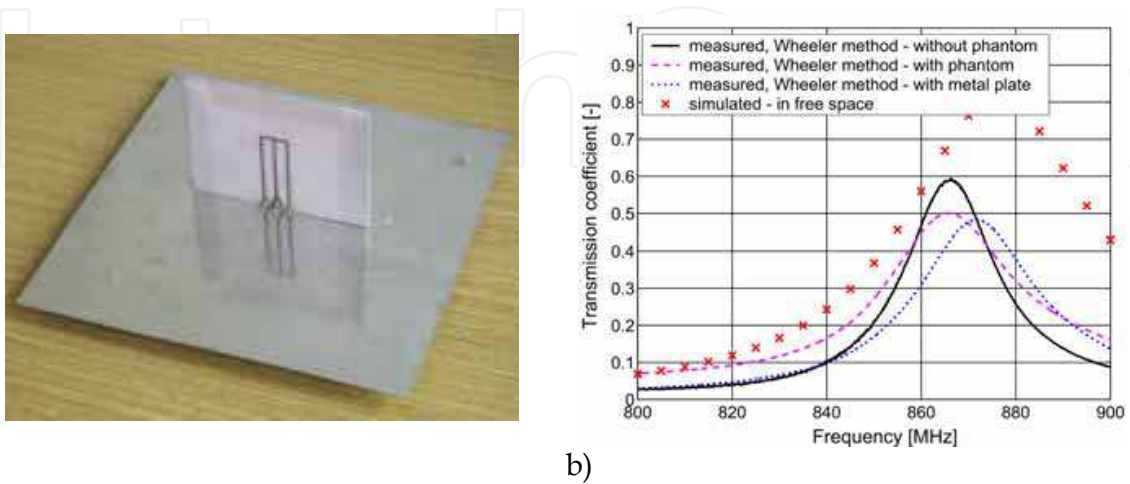
Fig. 11. The manufactured prototype of the half-loop arrangement a) photograph b) transmission coefficient related to the chip impedance.

The transmission coefficient (see Eq. 2) of the half-loop arrangement has been simulated and measured in free space, and on a human body phantom (agar with $\varepsilon_r \sim 55$ and $\tan\delta \sim 0.5$). The above-mentioned arrangement enables a measurement of the antenna and radiation efficiencies by means of the Wheeler cap method (Wheeler, 1959). The cap dimensions were $123 \times 123 \times 123$ mm. The measured and simulated values can bee seen in Fig. 12.

a)   b)
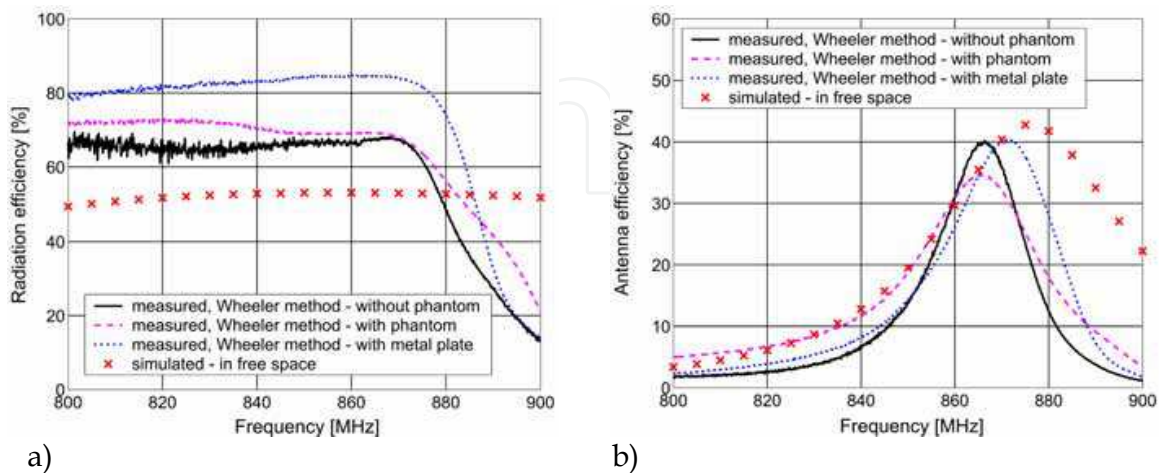
Fig. 12. Comparison of the simulated and measured a) radiation efficiency and b) antenna efficiency of the half dual-loop antenna depicted in Fig. 11.

The antenna gain has been evaluated from the measured antenna efficiency (Wheeler cap method) and directivity (evaluated from the measured radiation patterns). The simulated and measured antenna gain and directivity are summarized in Table 2.

	Radiation efficiency [%]	Antenna efficiency [%]	Directivity [dBi]	Gain [dBi]
Simulated, free space	53	39	5.3	1.3
Measured, free space	68	38	5.0	0.8
Measured, with agar	70	33	5.4	0.6
Measured, with metal	83	39	5.3	1.3

Table 2. The TAG antenna efficiency and gain simulated and measured in free space and in the close vicinity of the human body phantom at f = 869 MHz

The comparison between the simulated and measured radiation patterns can be seen in Fig. 13. Radiation patterns were measured using the dual-loop antenna fed by coaxial cable with the non-perfect symmetrization. That is why the E-plane pattern shows approx. 15° tilt which is not expected to be present in real TAG antenna-chip arrangement.

Dual-loop backed antennas can provide advantageous dimensions $0.2 \times 0.3 \times 0.005\ \lambda_0$ while having acceptable antenna efficiency and gain. They are supposed to be used in the form of a standard badge also bearing the person's photograph and name fixed on the chest; see Fig. 25. A minor disadvantage can be relatively higher weight caused by the usage of higher permittivity dielectric substrate.
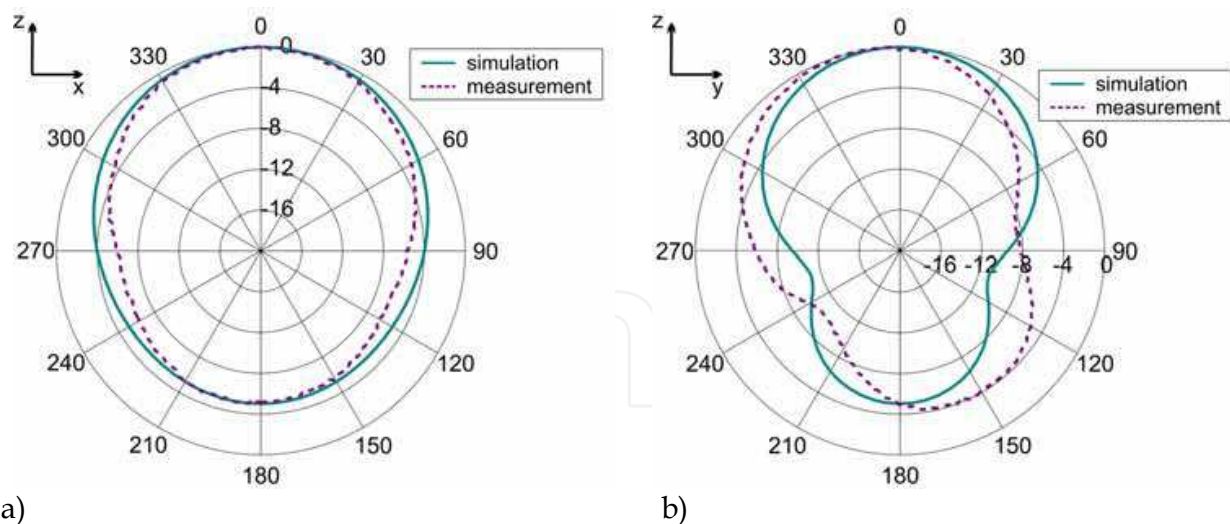
Fig. 13. The simulated and measured radiation patterns of the flat dual-loop antenna backed by the patch array surface a) H-plane b) E-plane.

3. Power budgets

The behavior and functionality of any RFID system based on electromagnetic wave coupling mechanism, used in the UHF and microwave frequency bands, depend substantially on wave propagation effects and the corresponding reader-TAG and TAG-reader power budgets. The P_{rTAG} TAG input power must be higher than the TAG sensitivity $P_{rTAGmin}$, which provides energy for modulation of the reflected wave. In the same way, in order to ensure correct data processing on the side of the reader, the input power of the reader receiver $P_{rREADER}$ must be higher than the reader sensitivity $P_{rREADERmin}$. These two conditions must be fulfilled simultaneously and define the expected identification area, described in a more detailed way in 3.2.

3.1 Propagation phenomena in UHF band

Propagation of electromagnetic waves between the reader and TAG antennas is influenced by several effects, namely by interference of direct and reflected rays, by waveguide effects, by mutual shadowing among persons in the irradiated area and by the possible tilt of the identified person. The first two items describe the principal propagation phenomena, the second two represent random effects. All of them can significantly affect the total loss between the reader and the TAG antenna and, therefore, the functionality of the whole RFID system. This problem must be solved by as precise as possible evaluation of all these influences. In the case of the principal propagation phenomena, they can be included in propagation models, see Sections 3.2 and 3.3. The influences of random effects are usually measured and compensated for by creating sufficient backups, both in the reader-TAG and TAG-reader power budgets.

3.2 Modeling of propagation in open areas

In the case of open areas, evaluations of reader-TAG and TAG-reader power budgets can be performed relatively simply by means of the analytical two-ray path-loss model. This commonly known model works with one direct ray and one ray reflected from the ground.

In order to improve the relation of the model with practical RFID arrangements, suitable modification was designed and verified (Švanda et al. 2007); see Fig. 14. The modification takes approximated 3D radiation patterns and general tilt of both the reader and TAG antennas into account. According to practical experience, the modified model provides a sufficient agreement between the measured and simulated data.

The propagation of an electromagnetic wave from the reader to the TAG can be described by means of the following path-loss formula:

$$L = -20\log\left(\left(\frac{\lambda}{4\pi}\right)\left|\sqrt{G_{tV}(\alpha_d)G_{rV}(\beta_d)G_{tH}(\gamma)G_{rH}(\delta)}\cdot\frac{1}{r_1}e^{-j\cdot k\cdot r_1} + \right.\right.$$
$$\left.\left. +\sqrt{G_{tV}(\alpha_r)G_{rV}(\beta_r)G_{tH}(\gamma)G_{rH}(\delta)}\cdot\overline{R}(\vartheta)\cdot\frac{1}{r_2}\cdot e^{-j\cdot k\cdot r_2}\right|\right) \tag{4}$$

where r_1, r_2 are the lengths of the direct and reflected rays, $G_{rV}(\beta)$, $G_{rH}(\delta)$ stand for the angular dependences of the gain of the reader antenna in the vertical and horizontal planes, $G_{tV}(\alpha)$, $G_{tH}(\gamma)$ represent the angular dependencies of the gain of the TAG antenna in the vertical and horizontal planes, $\overline{R}(\vartheta)$ is the complex reflection coefficient of the ground.
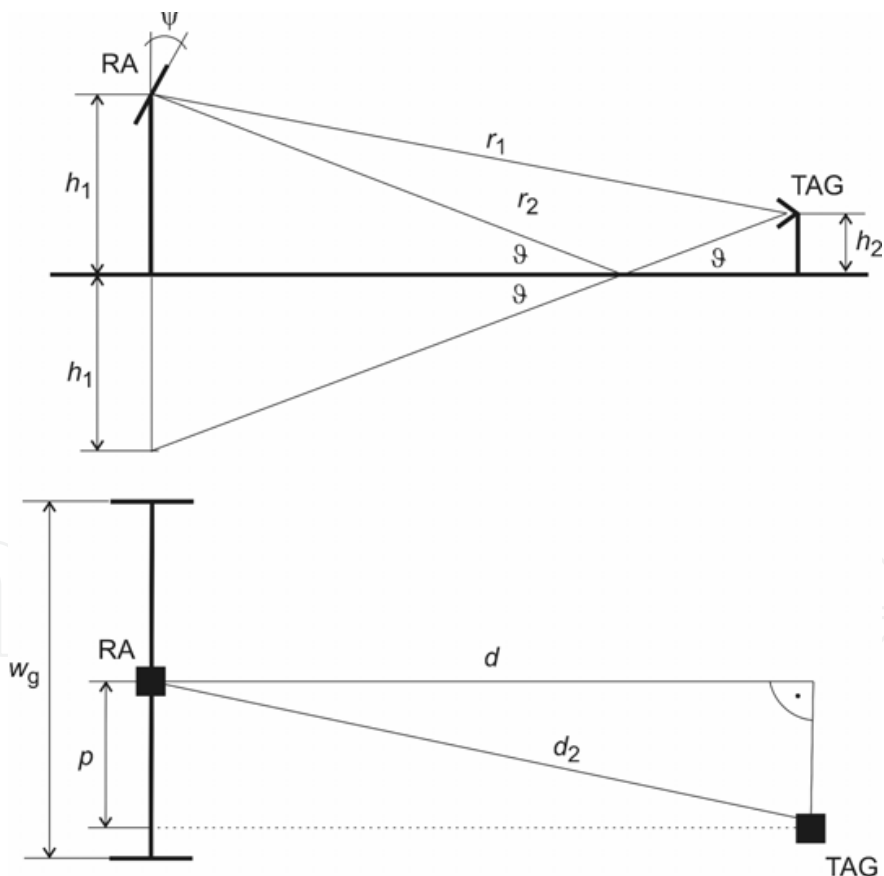

Fig. 14. Configuration of the two-ray model a) side-view b) top-view, with the following parameters: h_1 height of the reader antenna (denoted RA), h_2 height of the TAG antenna, r_1 direct ray length, r_2 reflected ray length, d_2 ground plane distance between the reader and TAG antennas, p reader and TAG antenna axis offset.

The P_{rTAG} power in dBm received by the TAG antenna can be expressed as follows:

$$P_{rTAG} = P_t - L - L_f \tag{5}$$

where P_t is the power in dBm transmitted by the reader, L stands for the path-loss and L_f represents the attenuation of the feeder cable in dB. The peak power of the modulated signal reflected back from the TAG and received by the receiver within the reader $P_{rREADER}$ in dBm can be expressed as follows:

$$P_{rREADER} = P_{rTAG} - L - L_f - L_{conv} \tag{6}$$

where L_{conv} is the conversion loss of the chip (typically 20 dB). The identification range can be defined as the area $\Delta d = d_{max} - d_{min}$ where d_{max} is the maximum identification distance and d_{min} is the minimum identification distance. Inside the identification range Δd, both received powers P_{rTAG} and $P_{rREADER}$ fulfill the following condition

$$P_{rTAG} \geq P_{rTAG\,min} \wedge P_{rREADER} \geq P_{rREADER\,min} \tag{7}$$
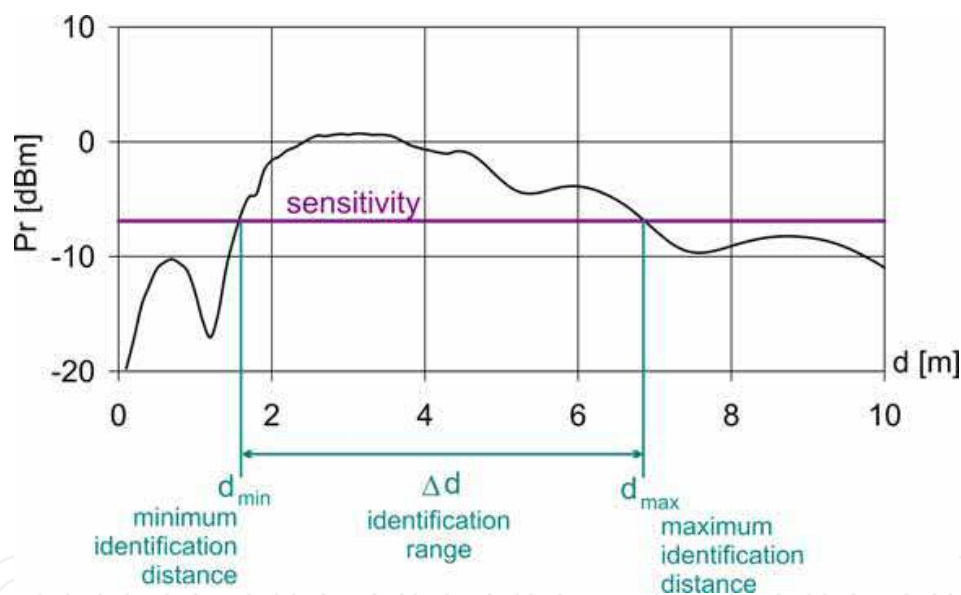
as can be seen in Fig. 15.

Fig. 15. Definition of the identification range

In order to cover the entire identification area, the identification range should be defined in more parallel lines with a p offset from the line axis. The reached values of the identification range Δd play an important role in the identification process. The reader can only perform a definite number (e.g. 70) of identifications per second. That is why the power budget conditions must be fulfilled for each TAG within a definite range Δd_{min} :

$$\Delta d_{min} = v_{max} / N_{rps} \tag{8}$$

Where v_{max} is the maximum expected speed of a moving person, N_{rps} is the identification rate (readings per second). For example, $v_{max} = 10$ m/s corresponding to a running person and $N_{rps} = 70$ lead to $\Delta d_{min} = 0.142$ m, the maximum expected speed of a cyclist

$v_{\max}$ = 20 m/s leads to Δd_{min} = 0.285 m. From this point of view, the system optimization must also be focused on ensuring enough high values of Δd with respect to Δd_{min}. The longer the Δd is, the higher the probability of the correct identification is, even under more difficult conditions. The higher Δd range also leads to a higher probability of the correct identification in the case where random effects (shadowing, tilt) are present also.

3.3 Modeling of propagation in indoor areas
The path-loss in indoor areas (typically corridors) is also influenced by waveguide effects. Attenuation of a field strength $E(r)$ is proportional to the term $(1/r)^n$ where n is a slope or path-loss exponent affected by the geometry of the corridor and electrical properties of the ground and ceiling, and side walls (Zvánovec et al. 2003). In this case, modeling the electromagnetic wave propagation is more complicated due to multiple reflections, diffractions around vertical wedges, and shadowing of walls and usually some form of a semi-analytical or numerical approach must to be used. For modeling path-loss in a long test corridor, a ray tracing method implemented in WinProp® software (by AWE Communication) was used. The method takes into account all propagation paths which fulfill the following criteria: up to 6 reflections, up to 2 diffractions, up to a total number of 6 interactions with a combination of max. 6 reflections and max. 2 diffractions. The particular ray tracing model uses coherent superposition and includes the real radiation pattern of the reader antenna. The radiation pattern of the receiving antenna is omnidirectional. Results show that waveguide effects in the corridor can increase the received power at the expected identification distance by constructive summation of direct, reflected and diffracted rays. The increased received power results in the increased identification range in corridors compared to open areas. In closed rooms resonant effects, both constructive and destructive summation must be expected.

3.4 Optimization of RFID systems for identification of people
As it has already been mentioned, in order to identify people each RFID system must be optimized or "tuned". The tuning should be focused especially on:
a. The selection of a suitable operating frequency and RFID system (reader, TAG chips). Low $P_{rTAGmin}$ and $P_{rREADERmin}$ values are beneficial.
b. The choice or design of suitable reader antennas, optimization of their positioning and tilt with respect to the identification area.
c. The choice or design of suitable TAG antennas. The most important features are immunity against the influence of the human body, small dimensions and weight.
d. The selection of a suitable propagation model, power budget calculations.
e. Practical verification of the propagation model used, measurement of possible random influences (shadowing, tilt), ensuring of required power backups.
f. Practical testing of the tuned system.
The following paragraphs describe an example of the optimization of a standard RFID system for identifying sportsmen during mass races.

3.4.1 Basic system and measurement configurations
The chosen RFID system operates at 869 MHz, its detailed parameters are described in Table 3. The system was optimized for identifying sportsmen during mass races, see (Švanda et al., 2007) and Fig. 14. It is a typical open area task, the sportsmen are supposed to pass through the checking or finishing gates equipped with TX and RX reader antennas.

The TAGs used must be very light and flexible, on the other hand, since they can be included in relatively large label numbers, they need not be extremely small. That is why the RFID patch TAG antennas described in Section 2.2 were used. The RFID system is supposed to read the identification numbers of all sportsmen in the race for checking purposes only. The measurement of time and precise succession of racers is ensured otherwise (for example by an optical camera).

For system optimization, a series of computer simulations and practical measurements was performed, see Fig. 16. The gate height was $h_1 = 3$ m, its width $w_g = 6$ m, the measurement TAG antenna was fastened on the chest of the test person at a height $h_2 = 1.3$ m. All measurements were performed for $d = 0 – 10$ m with a step 0.2 m and $p = 0 – 2.5$ m step 0.5 m, see Fig. 14. The gate was equipped with a TX reader antenna only. Since it was necessary to measure P_{rTAG} in wide dynamic ranges, a spectrum analyser with a standard $50\,\Omega$ input impedance was used. Consequently, it was necessary to face the fact, that the impedance of the TAG antenna is complex and different from $50\,\Omega$. The TAG antenna equipped with an impedance transformer or a special test antenna of the same type as the TAG antenna but with a $50\,\Omega$ output, was used.

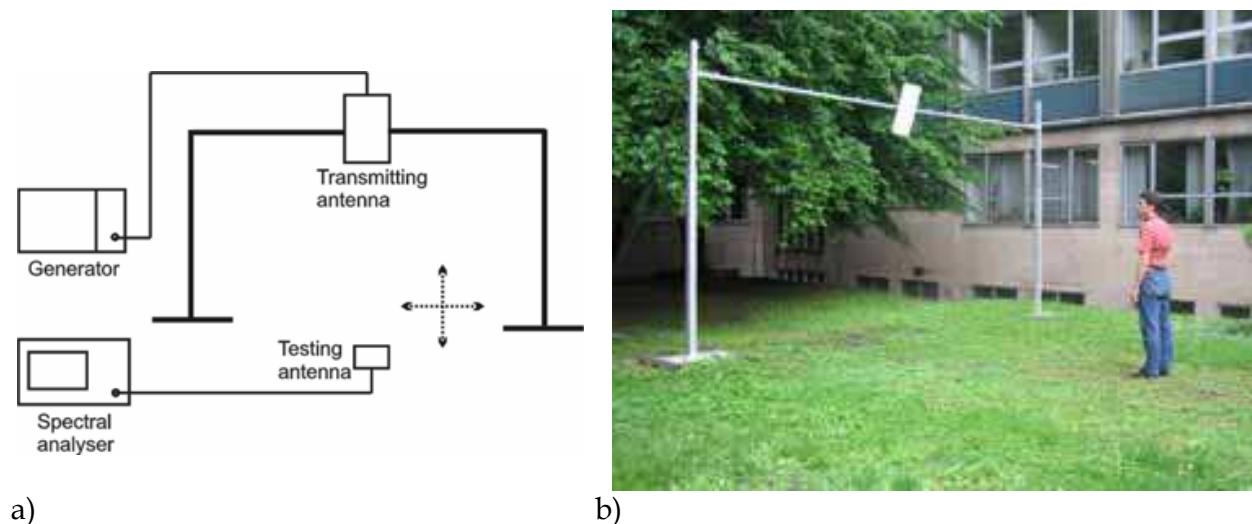a)   b)

Fig. 16. A practical measurement setup, a) scheme and b) a test person in front of a gate

3.4.2 New reader antenna

In order to enhance the effective radiated power of the transmitting antenna and to focus the energy to the expected identification area, the antenna with a microstrip patch collinear arrangement was used (Polívka et al., 2005). It provides a wide radiation pattern in the horizontal plane and narrower pattern in the vertical plane with a corresponding higher gain (11.7 dBi compared to 8.0 dBi of the original reader antenna). Fig. 17 shows its photograph and the measured radiation patterns. The same type was also used as the receiving antenna. The 3.7 dBi gain enhancement in both power budgets according to (5) and (6) was achieved.

3.4.3 Influence of tilt of the TX reader antenna

The first simulations were focused on finding the optimum tilt ψ of the reader antenna, see Fig. 14. Fig. 18 shows the simulation of the influence of ψ on the TAG input power P_{rTAG}.

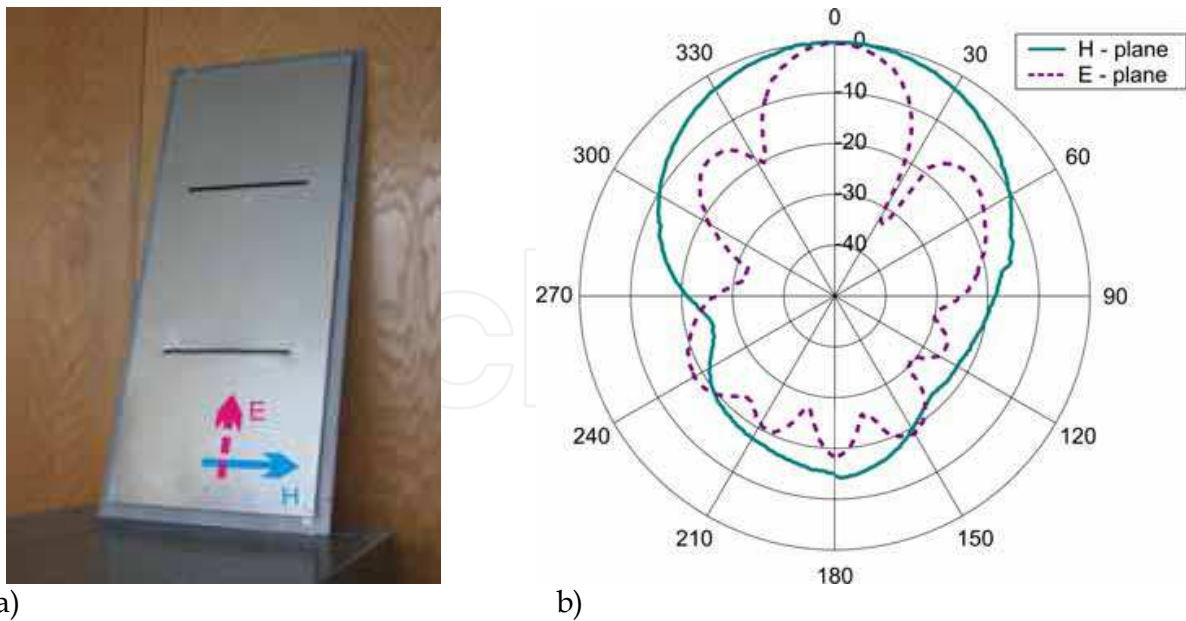a)   b)

Fig. 17. Photograph a) and measured radiation patterns b) of the new reader antenna

The plot indicates that the optimum tilt is $\psi = 30°$. Higher ψ values result in a steep P_{rTAG} decline in the $3 \leq d \leq 4$ m range, whereas a lower ψ value provides a low TAG input power in an important region $d < 4$ m close to the gate, where a smaller influence of the shadowing of TAGs by neighboring sportsmen can be expected. The difference between the maximum receiver power on the axis ($p = 0$ m) and off the axis ($p = 2.5$ m) is about 4 dB. The $\psi = 30°$ tilt was used for both other measurements and practical identification tests.

a)   b)
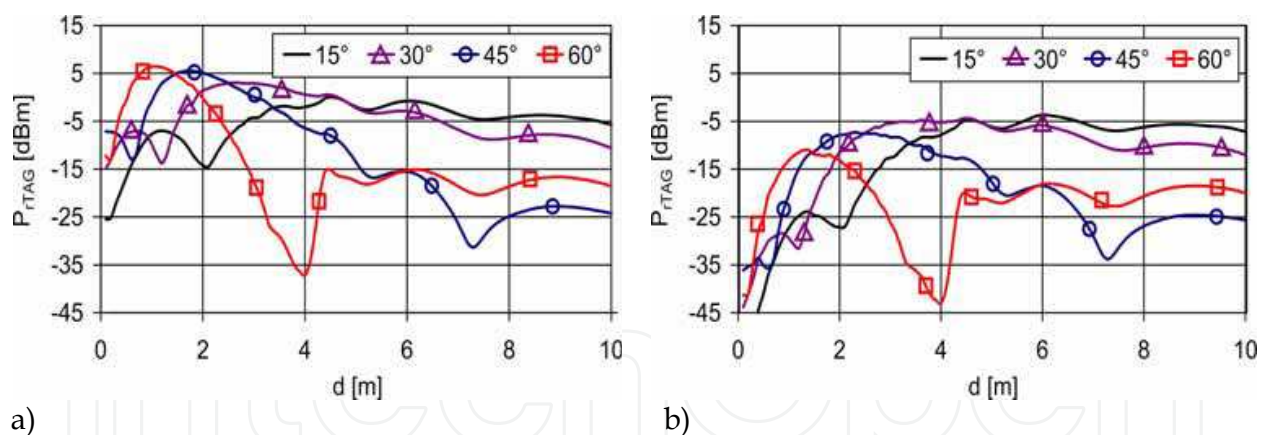
Fig. 18. Simulation of the TAG input power P_{rTAG} versus distance d for different tilt ψ of the reader antenna ($P_t = 35.4$ dBm, $h_1 = 3$ m, $h_2 = 1.3$ m) on the axis ($p = 0$ m) and off the axis ($p = 2.5$ m)

3.4.4 Influence of tilt of the TAG antenna

One possible additional loss can be caused by more or less random tilt of the TAG antenna caused by the natural tilt of a human body. It can be especially significant in the case of people running. These additional link losses were investigated by means of practical measurements in the arrangement according to 3.4.1.

Fig. 19 shows the measured P_{rTAG} values as a function of the distance d from the gate (on the gate axis $p = 0$) and tilt φ of the person. The presented data indicates that the tilt φ > 0 can

result in significant additional loss, especially in the ranges $d \leq 2$ m and $d > 7$ m. Nevertheless, in both of these regions, the simulated and measured P_{rTAG} values are below the $P_{rTAGmin}$ value even for $\varphi = 0$ (an erected person), and the identification is unlikely to be performed here. And on the contrary, the proper identification can be expected in the $2 \leq d \leq 7$ m range, where the influence of the person's tilt φ is relatively small and the additional loss caused by the tilt usually does not exceed 3 dB.
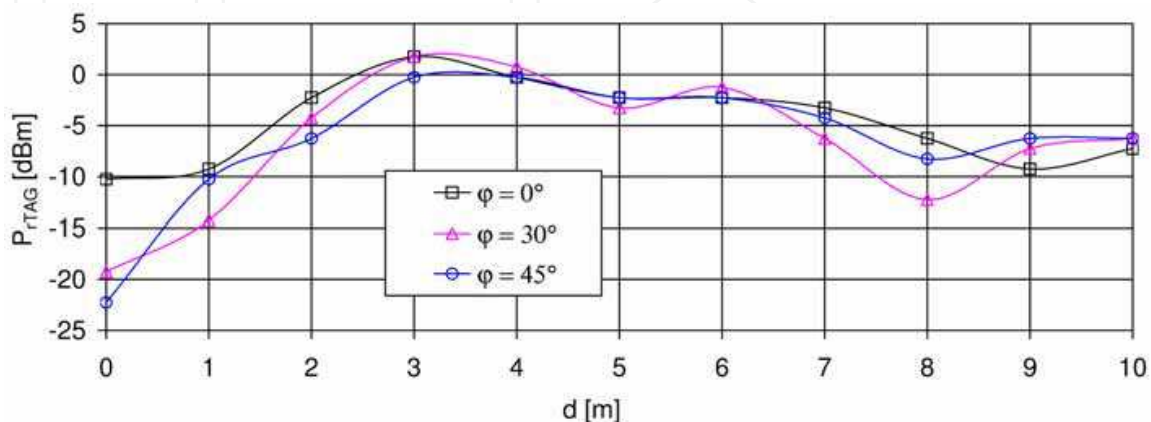
Fig. 19. Influence of tilt of a runner φ on the received TAG power P_{rTAG} (measurement, $P_t = 35.4$ dBm, $h_1 = 3$ m, $h_2 = 1.3$ m, $\psi = 30°$, $p = 0$ m)

3.4.5 Influence of mutual shadowing

If several people gather in a small area in an identification area, it may result in mutual shadowing and consequent additional path-loss. In practice, any configuration of people can appear. In order to get at least the basic information about this potential signal fading, a set of relatively simple measurements was performed. The P_{rTAG} values were measured at all positions described in 3.4.1 but one person was always standing erectly at a distance of 1 m in front of a person wearing the measurement antenna. The results of these measurements are presented in Fig. 20. As expected, the additional shadowing loss is strongly dependent on the distance d from the gate. Within the range $d \leq 3$ m, the influence of the shadowing is negligible. In the range between $3 \leq d \leq 5$ m, this shadowing loss is up to 3 dB, for $d > 5$ m the shadowing loss is around 6 dB.
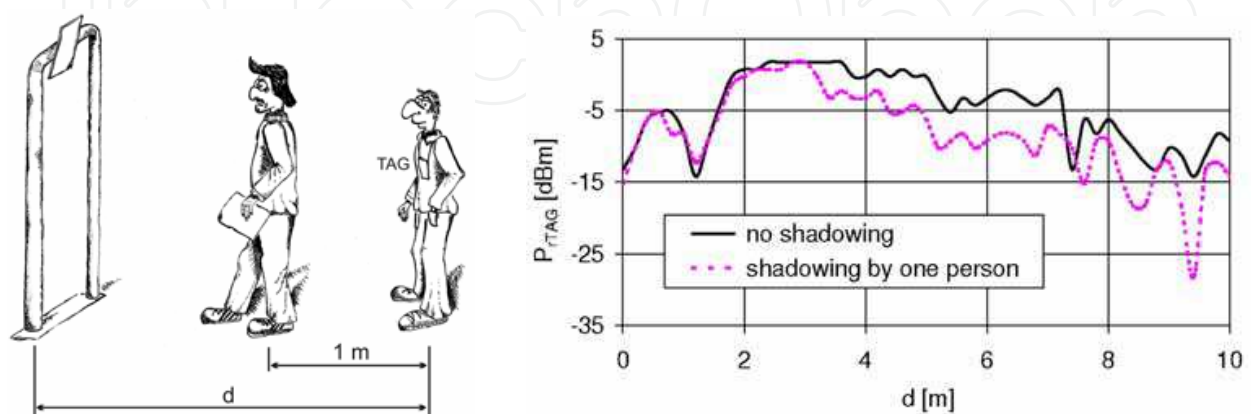

Fig. 20. Influence of shadowing on the TAG input power $PrTAG$ (measurement, $P_t = 35.4$ dBm, $h_1 = 3$ m, $h_2 = 1.3$ m, $\psi = 30°$, $p = 0$ m)

3.4.6 Power budgets of the optimized system

The following figures show the P_{rTAG} and P_{rREADER} plots as a function of distance d from the gate and p from the gate axis. To see the potential of the "tuning" procedure, the figures include the same dependencies measured with a standard meander dipole antenna (Polívka et al., 2006) fixed on a test person at a distance b = 20 mm without a screening metallic plate. Fig. 21 shows the plot of the simulated and measured TAG input power P_{rTAG} at the gate axis p = 0. Fig. 22 shows the simulated and measured P_{rTAG} values at the offset p = 2.5 m. Both figures include the corresponding $P_{\text{rTAG}min}$ sensitivity value and compare the results obtained from the new RFID patch and the standard meander dipole. With the meander dipole antenna used, the P_{rTAG} values are above the $P_{\text{rTAG}min}$ for p = 0 m, but with only 3 dB backup. For p = 2.5 m, P_{rTAG} is significantly below $P_{\text{rTAG}min}$. That is why a non optimized system can only work close to the gate axis and with low identification reliability; see Table 4. The optimized system show min. 6 dB backup even at the p = 2.5 m offset. That is why its identification reliability is 100 % in the entire required identification area and even under worst expected conditions; see Table 4.
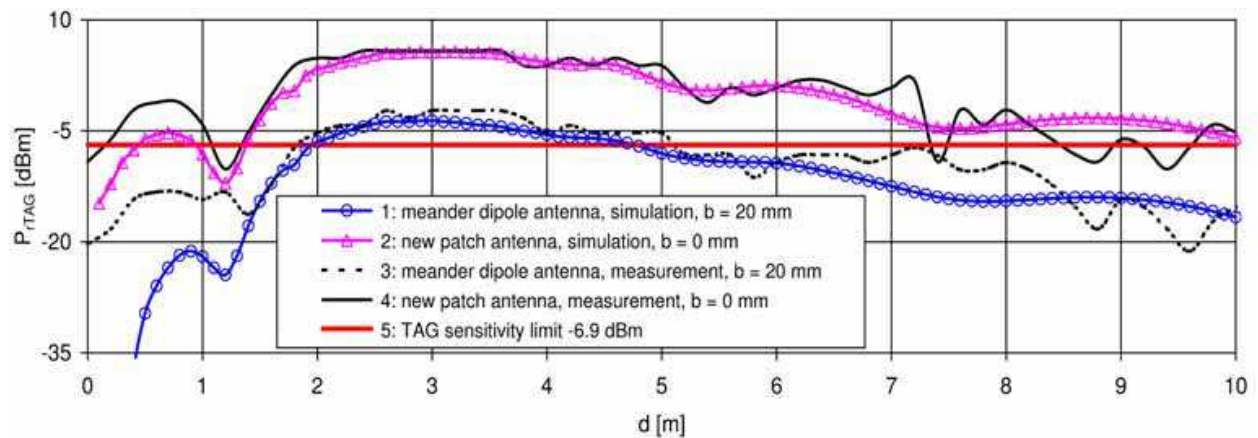

Fig. 21. Simulated and measured TAG input power P_{rTAG} on the reader-TAG trace
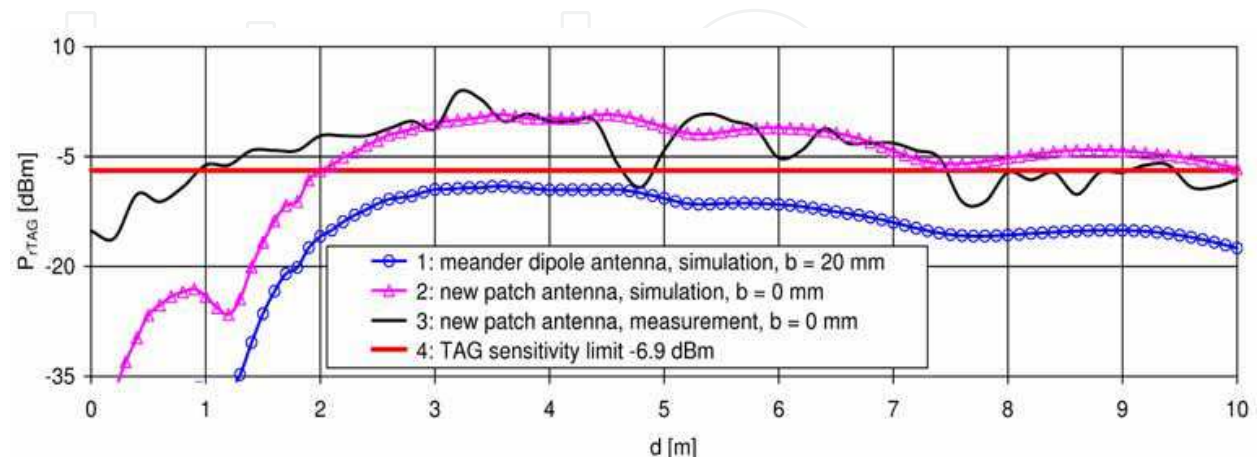(P_t = 35.4 dBm, h_1 = 3 m, h_2 = 1.3 m, ψ = 30°, p = 0 m)

Fig. 22. Simulated and measured TAG input power P_{rTAG} on the reader-TAG trace
(P_t = 35.4 dBm, h_1 = 3 m, h_2 = 1.3 m, ψ = 30°, p = 2.5 m)

Fig. 23 shows the simulated reader input power $P_{rREADER}$ values with respect to the reader sensitivity $P_{rREADERmin}$. Use of the standard meander dipole antenna leads to unacceptably low $P_{rREADER}$ values, especially off-axis. Employment of the RFID patch, optimized for operation on a human body, can guarantee high enough power even in this return TAG-reader link.
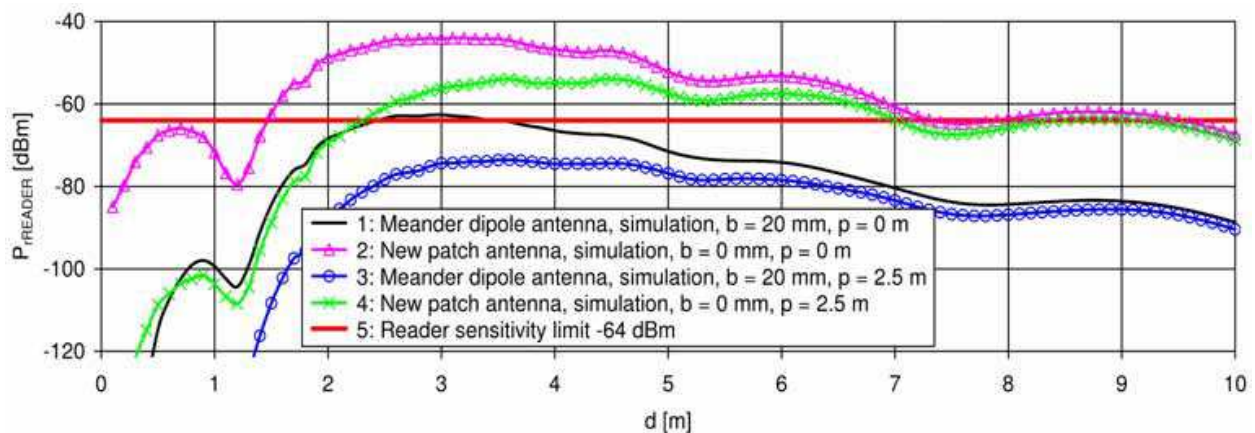

Fig. 23. Simulated reader input power $P_{rREADER}$ on the TAG-reader trace (P_t = 35.4 dBm, h_1 = 3 m, h_2 = 1.3 m, ψ = 30°)

4. Testing of RFID systems

According to 3.4 f) it is always necessary to perform practical testing of the optimized RFID system. As examples, testing of two RFID systems optimized for different applications are presented. The first system was optimized for identification of sportsmen; see Section 3.4. The second system was tuned for identification of employees in buildings and factory areas. Both arrangements employ the same reader and TAG chips.

4.1 Description of the RFID reader and chips
For the identification tests, a commercial RFID system (Trolleyscan Ltd, 2006) operating in the 869 MHz band was used. The main parameters of the system can be seen in Table 3.

System components	Parameter	Values
	Operating frequency (Europe)	869.5 – 869.7 MHz
Reader	Transmitted power	24.7 dBm – 36.0 dBm
	Receiver sensitivity	-64 dBm (200 pW)
	Identification rate	70 s⁻¹
Chip	Sensitivity	-6.9 dBm (200 µW)
	Impedance (measured value)	76 - j340 Ω
	Conversion loss	approx. 20 dB

Table 3. Standard UHF RFID system parameters, from (Trolleyscan Ltd, 2006)

4.2 Identification of sportsmen

In order to verify identification reliability of the optimized system, tests simulating real RFID system applications were performed. A group of racers moved on an asphalt surface in several different formations, see Fig. 24. In the first formation, 7 racers moved in a row, in the second formation 7 racers formed a kind of a matrix. Each formation moved with 3 different speeds simulating a walk (approx. 4 km/h), a fast walk (approx. 8 km/h) and a run (approx. 15 km/h). Each test was repeated 3 times. For comparison, tests were performed using both the RFID patch and standard planar dipole TAG antennas fixed on thick foam spacer (b = 20 mm). The results of performed tests are presented in Table 4.
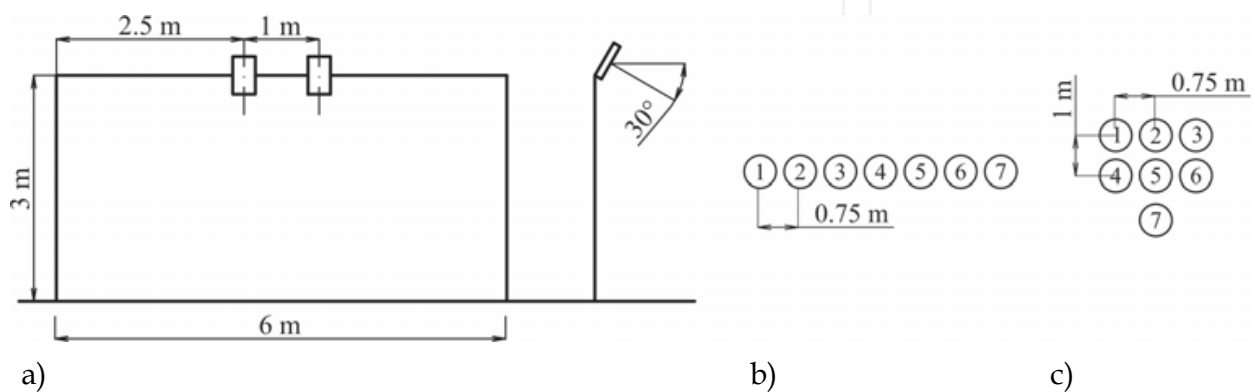
Fig. 24. Antenna gate dimensions a) and basic formations of racers used for testing of the optimized RFID system in a b) row, c) matrix

Configuration of racers	Speed of racers	Percentage of correct identification	
		Dipole antenna	RFID patch ant.
row	walk	66.7 %	100 %
	fast walk	52.4 %	100 %
	run	-	100 %
matrix p = 2.5 m	walk	61.7 %	100 %
	fast walk	52.4 %	100 %
	run	-	100 %
matrix p = 0 m	walk	85.7 %	100 %

Table 4. Reliability of identification of racers in open area obtained with dipole and the RFID patch TAG antennas

The presented results show that the optimization of the RFID system according to Section 3.4 can guarantee 100 % identification reliability, even under the worst expected conditions (shadowing tilt).

4.3 Identification of employees

The second test scenario was focused on identifying employees in buildings and factories; see (Polívka et al., 2008b). Identification tests were performed both in corridors and open areas in front of a building; see Fig. 25. Badge-type dual-loop TAG antennas, see Section 2.3, fixed on a person's chest and smaller 8 dBi reader antennas were used.

During these identification tests, values of the maximum identification distance $d_{\max}$ were measured. In order to enable comparison of the measured and expected $d_{\max}$ values, computer simulations of $P_{rTAG} = f(d)$ and $P_{rREADER} = f(d)$ were added; see Fig. 26 and Fig. 27. The $d_{\max}$ values are defined here as the most distant point where (7) is fulfilled.
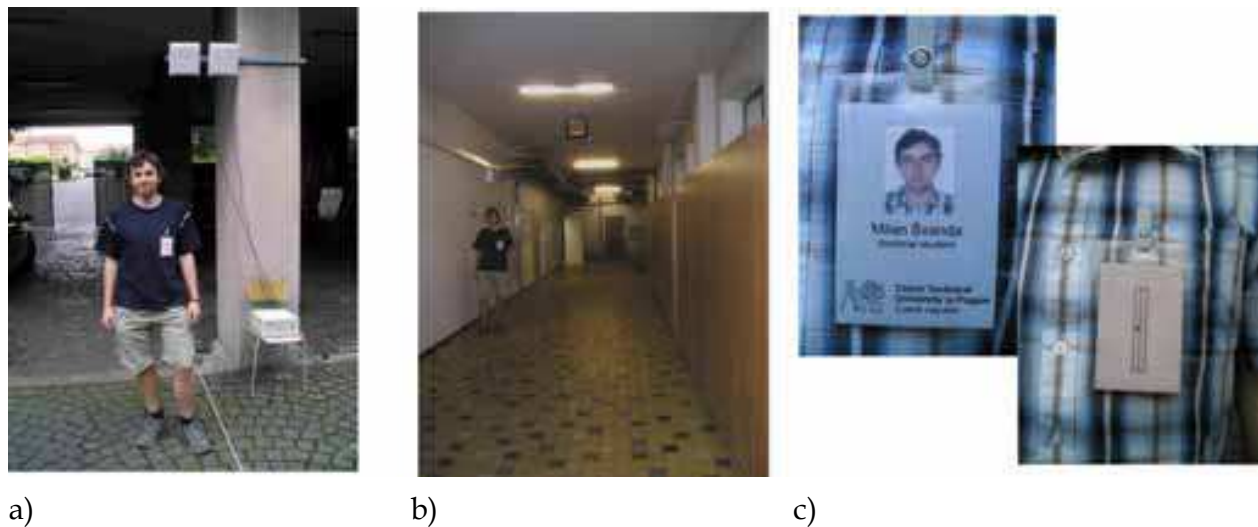

a)   b)   c)

Fig. 25. Photograph of person with chest-fixed TAG in a) an open area and b) a corridor c) detail of TAG

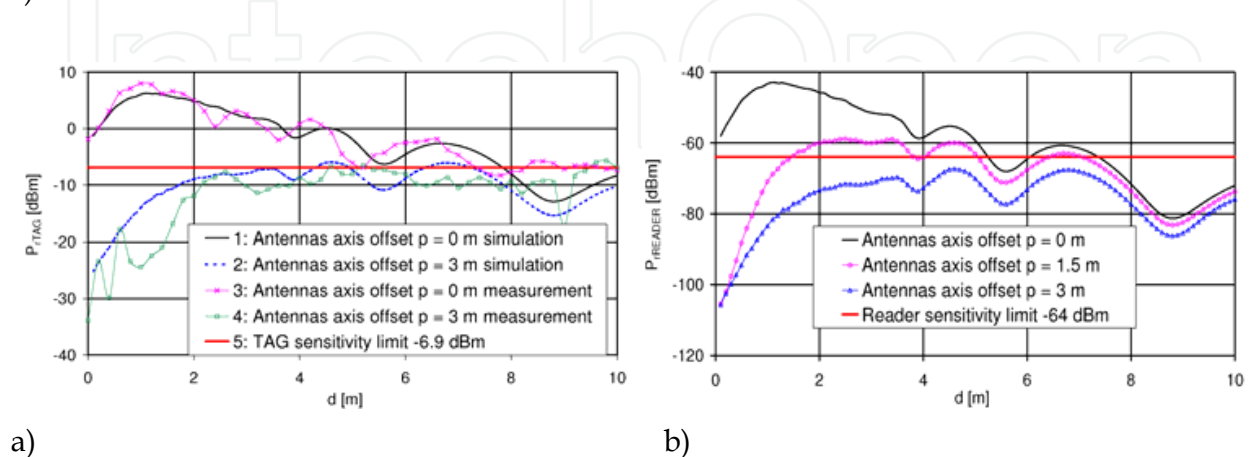a)   b)

Fig. 26. Simulation of the received power P_{rTAG} (a) and $P_{rREADER}$ (b) versus distance d ($P_t = 35.4$ dBm, $h_1 = 2.5$ m, $h_2 = 1.25$ m, $\psi = 30°$).

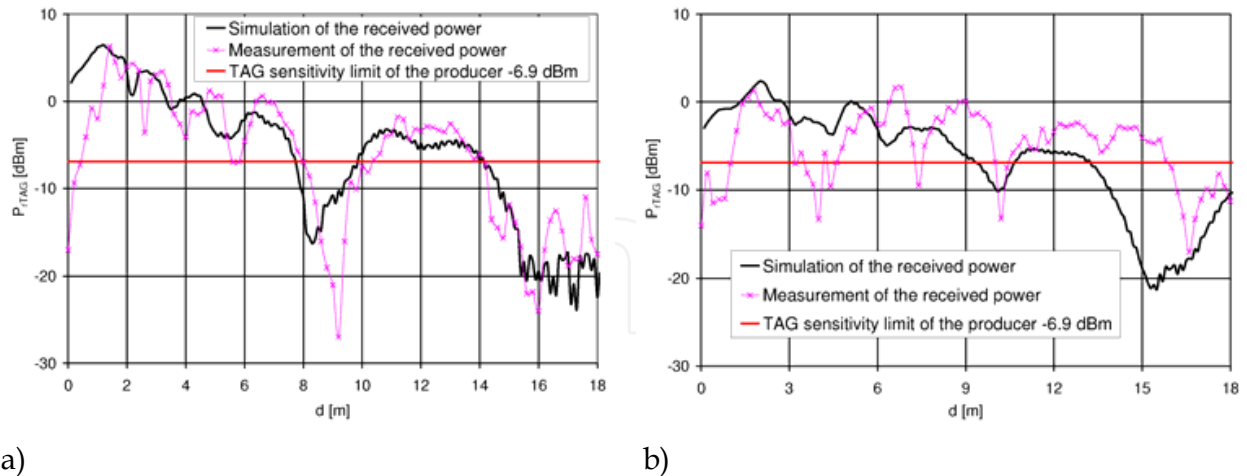a)   b)

Fig. 27. Simulated (3D ray tracing) and measured received power P_{rTAG} versus base antenna distance (P_t = 35.4 dBm, h_1 = 2.5 m, h_2 = 1.25 m, ψ = 30°) in case of persons identification in corridor. (a) In the axis p = 0 m, (b) in the antennas axis offset p = 1.8 m

Position of TAG antenna	Reader and TAG antenna axis offset - p [m]	Max. identification distance - d_{max} [m]
Person's chest, open area	0	9
	1	6.5
	2	4
	3	unreliable id.
Person's chest, 4 m wide corridor	0	9
	1	8
	1.8	8

Table 5. Maximum identification distance of test configurations

The measured d_{max} values are presented in Table 5. The agreement between the measured and simulated values is very good.

5. Conclusion

Reliable RF identification of people in moderate 2 – 10 m ranges must be based on electromagnetic wave coupling mechanism. Due to acceptable antenna dimensions, UHF or microwave operational frequencies must be used. At these frequencies, propagation of electromagnetic waves is influenced by several important physical phenomena, namely by interferences, shadowing or waveguide effects. Besides these, in this application, the functionality of TAG antennas can be negatively influenced by the presence of a nearby

human body. The human body is able to detune definite antenna structures and to absorb a substantial part of the radiated or received signal power. All these effects can lead to the wrong or even no identification.

In order to guarantee reliable identification, the whole UHF RFID system must fulfil power budget conditions, both in the reader-TAG and TAG-reader radio paths. These conditions compare power levels received by the TAG and reader antennas with reader and TAG sensitivities. Primarily, power budgets are influenced by radiated power, gains of all antennas and by propagation loss. Beside these, several additional random attenuations of electromagnetic waves must be taken into account. Above all this concerns the tilt of the TAG antenna caused by the possible tilt of the person to be identified and by shadowing among persons in a group in an identification area. These additional random losses should be measured and added into power budget calculations as necessary reserves.

In order to reliably fulfil both power budget conditions, each RFID system intended for identification of people should be "tuned". Above all, this concerns both TAG and reader antennas. The TAG antennas must be as lightweight and small as possible, and must especially provide high immunity against the influence of a nearby lossy dielectric. Employment of antenna structures with metallic planes can be recommended. The metallic planes can form a mere screening or can form inherent parts of the antennas. In case of reader antennas, optimization of their beam shapes and tilt can also be very beneficial.

Two examples of RFID systems "tuned" for different purposes were presented. The first system was optimised for identification of runners in long-distance races. Initial tests using standard TAG and reader antennas provided unacceptably low identification probability (around 50 %). Designing new TAG and reader antennas and changing the system arrangements led to a 100 % identification probability in the whole required identification area under the expected rugged conditions. Similar power budget calculations and optimization steps were performed in the second system intended for identification of personnel in buildings or areas. The optimization was focused on designing a new TAG antenna with dimensions comparable with a standard photo and name bearing identification badge. Practical tests show, that this system is able to identify people walking in 4 m wide corridors or 5 m wide strips in open areas, in both cases the maximum available identification range is around 9 m. A suitable combination of open-area and corridor readers can cover the majority of standard buildings or nearby areas. The UHF RFID system can help with the organization of mass events or provide security information and services in many offices, warehouses or factories. All that without much inconvenience to personnel or time delays.

6. Acknowledgement

7. References

Balanis, C. A. (1997). *Antenna Theory, Analysis and Design*, second edition, John Wiley & Sons, ISBN 0-471-59268-4, New York

Best, S. (2004). Improving performance properties of a dipole element closely spaced to a PEC ground plane. *IEEE Antennas and Wireless Propagation Letters*, Vol. 3, 2004, pp. 359-363, ISSN 1536-1225

Dobkin, D. M. & Weigand, S. M. (2005). Environmental effects on RFID TAG antennas, *Proceedings of IEEE Antennas and Propagation Society International Symposium 2005*, ISBN 0-7803-8845-3, Washington, USA, July 2005

Finkenzeller, K. (2003). *RFID Handbook: Fundamentals and Applications in Contactless Smart Cards and Identification*, 2nd edition, John Wiley & Sons, ISBN 0-470-844402-7, Chichester

Foster, P. R. & Burberry, R,. A. (1999). Antenna problems in RFID systems, *Proceedings of IEE Colloquium RFID Technology*, pp. 31-35, London, UK, October 1999

Gautherie, M (1990). *Biological Basis of Oncologic Thermotherapy*, Springer-Verlag, Conference, Berlin

Griffin, J. D.; Durgin, G. D.; Haldi,A. & Kippelen, B. (2006). RF TAG antenna performance on various materials using radio link budgets. *IEEE Antennas and Wireless Propagation Letters*, Vol. 5, 2006, pp. 247-250, ISSN 1536-1225

Hansen, R. C. (2006). *Electrically Small, Superdirective, and Superconductive Antennas*, John Wiley & Sons., ISBN 0-471-78255-6, New York

Lee, K. F. & Chen, W. (1997). *Advances in Microstrip and Printed Antennas*, John Wiley & Sons, ISBN: 978-0-471-04421-5, New York

Noguchi, K.; Syouji, H.; Mizusawa, M.; Yamaguti, T. & Okumura, Y. (1997). Impedance characteristics of small meander line antenna. *Technical report of IEICE*, pp 97-55, 1997

Polívka, M.; Holub, A. & Mazánek, M. (2005). Collinear Microstrip Patch Antenna. *Radioengineering*, Vol. 14, No. 4, 2005, p. 40-42. ISSN 1210-2512

Polívka, M.; Švanda, M. & Hudec, P. (2006). Analysis and Measurement of the RFID System Adapted for Identification of Moving Objects., *Proceedings of the 36th European Microwave Conference* [CD-ROM], pp. 729-732, ISBN 2-9600551-6-0, Manchester, October 2006, Piscataway: IEEE

Polívka, M.; Švanda, M. & Černý, P. (2008a). Multiple-Arm Folded Monopole Antenna Operating Extremely Close to a Conductive Plane, *Proceeding of COMITE 2008*, pp. 61-65, ISBN 978-1-4244-2137-4, Prague, May 2008, Czechoslovakia Section IEEE, Prague

Polívka, M.; Švanda, M. & Hudec, P. (2008b). UHF radiofrequency identification of persons in buildings and open areas. Submitted to *Transaction on Microwave Theory and Technique, Special Issue on Hardware and Integration Challenges of RFID's*, ISSN 0018-9480

Ranasinghe, D. C., Hall, D. M., Cole, P. H., Engels, D. W. (2004). An embedded UHF RFID label antenna for TAGging metallic objects, *Proceeding of Inteligent Sensors, sensor Networks and Information Processing Conference*, pp. 343 – 347, ISBN 0-7803-8894-1, December 2004

Raumonen, P., et al. (2003). Folded dipole antenna near metal plate, *Proceedings of IEEE Antennas and Propagation Society International Symposium 2003*, pp. 848-851, ISBN 0-7803-7846-6, June 2003

Sidén, J.; Nilsson, H.-E., Koptyug, A. &, Olsson, T., (2006). A Distanced RFID dipole for a metallic supply chain label, *Proceedings of IEEE Antennas and Propagation Society International Symposium 2006*, pp. 3229 – 3232, Albuquerque, New Mexico, July 2006

Sievenpiper, D. (1999). *High-impedance electromagnetic surfaces*, Ph.D. dissertation, Department of Electrical Engineering, University of California at Los Angeles, Los Angeles

Švanda, M.; Polívka, M. & Hudec, P. (2007). Application of the UHF RFID system for the identification of sportsmen in mass races, In: *Proceedings of the European Microwave Association*. Vol. 3, No. 4 (December, 2007), pp. 295-301, Edizioni Plus - Universita di Pisa, ISBN 88-8492-324-7, Pisa

Švanda, M. & Polívka, M. (2007). Dualband wearable UHF RFID antenna, *Proceeding of the 2nd European Conference on Antennas and Propagation* [CD-ROM], pp. 1-5, ISBN 978-0-86341-842-6, Edinburgh, October 2007, Stevenage, Herts: The Institution of Engineering and Technology (IET), Edinburgh

Švanda, M. & Polívka, M. (2008). Novel dual-loop antenna placed over patch array surface for UHF RFID of dielectric and metallic objects. Submitted to *Microwave and Optical Technology Letters*, ISSN 0895-2477

Trolleyscan, Ltd. (2006). http://www.trolleyscan.com/, 5. 6. 2006

Ukkonen, L. & Kivikoski, P. R., (2003). Challenges in the development of TAG antennas for passive RFID of metallic objects, *Proceedings of IV Finnish Wireless Communications Workshop*, October 2003

Ukkonen, L.; Engles, D. ; Sydanheimo, L. & Kivikoski, M. (2004). Planar wire-type inverted-F RFID TAG antenna mountable on metallic objects, *Proceeding of IEEE Antennas and Propagation Society International Symposium 2004*, pp. 101-104, Monterey, California, June 2004

Ukkonen, L.; Sydänheimo, L. & Kivikoski, P. R. (2005). Effects of metallic plate size on the performance of microstrip patch-type TAG antennas for passive RFID. *IEEE Antennas and Wireless Propagation Letters*, Vol. 4, 2005, pp. 410 – 413, ISSN 1536 – 1225

Wheeler, H. A. (1959). The radian sphere around a small antenna. *Proceedings of IRE*, (August 1959), pp. 1325 –1331

Zhang, Y.; Hagen, J. et al. (2003). Planar artificial magnetic conductors and patch antennas. *IEEE Transactions on Antennas and Propagation*, Vol. 51, No. 10, (October 2003), pp. 2704-2712, ISSN 0018-926X

Zvánovec, S., Pechač P. & Klepal M. (2003). Wireless LAN Networks Design: Site Survey or Propagation Modeling?. *Radioengineering*, Vol. 12, No. 4, (December 2003), pp. 42-49, ISSN 1210-2512

Development and Implementation of RFID Technology

Edited by Cristina Turcu

The book generously covers a wide range of aspects and issues related to RFID systems, namely the design of RFID antennas, RFID readers and the variety of tags (e.g. UHF tags for sensing applications, surface acoustic wave RFID tags, smart RFID tags), complex RFID systems, security and privacy issues in RFID applications, as well as the selection of encryption algorithms. The book offers new insights, solutions and ideas for the design of efficient RFID architectures and applications. While not pretending to be comprehensive, its wide coverage may be appropriate not only for RFID novices but also for experienced technical professionals and RFID aficionados.

How to reference

In order to correctly reference this scholarly work, feel free to copy and paste the following:

Milan Polívka, Milan Švanda and Přemysl Hudec (2009). UHF RFID of People, Development and Implementation of RFID Technology, Cristina Turcu (Ed.), ISBN: 978-3-902613-54-7, InTech, Available from: http://www.intechopen.com/books/development_and_implementation_of_rfid_technology/uhf_rfid_of_people

INTECH
open science | open minds